NASA TM X-1483

PRELIMINARY INFRARED HORIZON PROFILES FROM PROJECT SCANNER

By Thomas B. McKee, Ruth I. Whitman,
and Richard E. Davis

Langley Research Center
Langley Station, Hampton, Va.

NATIONAL AERONAUTICS AND SPACE ADMINISTRATION

For sale by the Clearinghouse for Federal Scientific and Technical Information
Springfield, Virginia 22151 – CFSTI price $3.00

PRELIMINARY INFRARED HORIZON PROFILES FROM PROJECT SCANNER

By Thomas B. McKee, Ruth I. Whitman,
and Richard E. Davis
Langley Research Center

SUMMARY

Measured horizon radiance profiles in spectral bands of 615 cm^{-1} to 715 cm^{-1} (CO_2) and 315 cm^{-1} to 475 cm^{-1} (H_2O) from Project Scanner flight of August 16, 1966, are shown. Excellent agreement between measured and analytically predicted radiance profiles in the CO_2 region verifies the analytical technique to within the experimental accuracy. The agreement of measured with predicted profiles and the lack of dependence on presence of clouds indicate the 615 cm^{-1} to 715 cm^{-1} region is a good candidate for use in attitude determination applications. Horizon profiles in the 315 cm^{-1} to 475 cm^{-1} region show a strong dependence on the presence of clouds which indicates that the spectral region would be a poor one for attitude determination applications.

INTRODUCTION

From the beginning and throughout the growth of space technology, systems have employed horizon sensing techniques where the earth's limb or horizon was sensed to determine the attitude of a spacecraft. The desire for these devices to operate during both the day and night led to sensors in the infrared region of the spectrum where the horizon characteristics are produced by the contrast of the "cold" of space with the thermal emissions of the earth and its atmosphere. Flight experiences revealed operational problems with first-generation horizon scanners which were identified as being due to high, cold clouds. It was then recognized that selection of the spectral region could reduce the effects of clouds and other variabilities in the horizon profile characteristics. Spectral regions containing two strong absorption bands of atmospheric constituents, carbon dioxide and water vapor, have been identified as potentially the most useful for horizon scanning purposes. Horizon radiance profiles computed for the 665 cm^{-1} (15μ) CO_2 band and for parts of the extensive rotational water vapor band (wavelengths greater than about 17μ) for several atmospheres are discussed in references 1, 2, and 3. The CO_2 band appears the more promising because CO_2 has a known constant mixing ratio in the atmosphere, and it absorbs strongly enough to limit the effects of clouds and the variable lower atmosphere. A detailed analytical study of the

horizon characteristics in this CO_2 band is given in reference 4. Water vapor is considered because it is a strong absorber and is active over a wide spectral range. The H_2O mixing ratio however is variable with altitude and time, which would cause significant variations in the horizon profiles.

Experimental measurement of horizon profiles (horizon radiance as a function of tangent height or angle) in the 15μ CO_2 band and rotational H_2O band with sufficient optical resolution to observe horizon features is reported in references 5, 6, and 7. Data in reference 5 were taken with a 14μ to 20μ filter and therefore included both CO_2 and H_2O emissions. Reference 6 reports data for the 15μ CO_2 band and the 20μ to 35μ portion of the H_2O band; however, the position of the radiance profiles relative to the solid earth is not clear. Initial data from Project Scanner are given in reference 7 for the CO_2 band (615 cm^{-1} to 715 cm^{-1}) and for a region in the H_2O band (315 cm^{-1} to 475 cm^{-1} or about 21μ to 32μ).

Project Scanner has performed two flight experiments, the first on August 16, 1966, and the second on December 10, 1966. This preliminary report presents only a few example radiance profiles from the August flight. These profiles illustrate the variations experienced over the latitude range covered by this flight during a summer condition. Analytical radiance profiles in the CO_2 band based on meteorological data taken near the time of the experiment are also presented and compared with the measured data.

SYMBOLS

h	altitude, km
H	tangent height, km (see fig. 8)
k	radiance responsivity, volts-meters^2-steradian per watt
N	radiance, watts per meter^2-steradian
$N_{\bar{\nu}}$	spectral radiance, watts per meter^2-steradian-centimeter^{-1}
r	radius of earth, kilometers
T	temperature, degrees Kelvin
V	signal, volts
ρ	reflectance of calibrator optics, unitless

σ standard deviation

φ radiometer spectral response, unitless

$\bar{\nu}$ wave number, centimeter^{-1}

DESCRIPTION OF EXPERIMENT

Horizon radiance profiles have been measured with instrumentation on a modified Trailblazer II launch vehicle which was launched from the NASA Wallops Station at 0618 GMT on August 16, 1966. After staging and exiting the atmosphere the spacecraft was despun to 300 deg/sec and erected to within 2° of the local vertical by a cold gas reaction jet system which derived information from a horizon sensor and rate gyro (ref. 8). Data collection began at an altitude of 430 km, continued through apogee at 620 km, and down to 350 km with three brief interruptions to reerect the spacecraft. Horizon profile scans in the vertical were produced by scanning mirrors in the dual radiometer.

Dual Radiometer

A sketch of the dual radiometer used is shown as figure 1. The dual radiometer is actually two similar radiometers mounted back to back looking out in opposite directions. One side operates in the spectral region of CO_2 emission and the second in the H_2O region. For each radiometer a flat scanning mirror provides the vertical scan motion at 10 deg/sec over a total angle of 15° and directs the incoming radiation into the optical system which has an entrance aperture of 23 cm in diameter and a focal length of 33 cm. An image is formed in the focal plane where a field stop determines the shape of the field of view. Five separate fields of view are formed by the field stop. Each one is nominally 0.025° in the vertical, 0.10° in the horizontal, and separated by 0.15° in the vertical. An immersed thermistor bolometer detector is located behind each opening in the field stop and data are telemetered continuously from all five detectors. Detector choice and scan rate prevent chopping in the radiometer.

A spectral filter is located before the field stop in each radiometer and is therefore common to all five detectors. The filter for the CO_2 band is an interference filter with substrates of germanium and pressed sintered zinc selenide. Detectors are immersed under germanium. The spectral response was determined for each channel by combining measurements of filter, detector, and optics; a typical one is shown in figure 2. A representative field of view is shown in figure 3. An example of frequency characteristics, amplitude ratio and phase angle, is given in figure 4. The electrical bandwidth at -3 dB point for the CO_2 side is 0.16 Hz to 38 Hz.

In the H_2O band radiometer, the filter has an interference coating on silicon for a cut-on and potassium bromide for a cut-off. Detectors are immersed under silicon. The spectral response, field of view, and frequency data are given in figures 2, 5, and 6. Bandwidth at -3 dB point for the H_2O side is 0.16 Hz to 39 Hz.

As the mirror scans, angular position relative to the spacecraft is determined with four points along the 15^o linear scan. The times when the mirror passes these four locations are telemetered in order that the mirror position at any other time may be computed.

Star Mapper

Inertial attitude of the spin-stabilized spacecraft was determined from measurements furnished by a star mapper which was mounted on top of the radiometer and whose optical alinement with the radiometer was very precisely measured. A sketch of the star mapper, which is a wide-angle, high-resolution star telescope, is shown as figure 7. Light entering the entrance aperture is imaged on a coded reticle located in the focal plane. Light passing through the reticle is diffused over the surface of the cathode of a photomultiplier tube. On the opaque reticle are located two groups of transparent slits. Spacing or coding of each group is a necessary aid in star detection. One group of slits is parallel to the spin axis, and the other group is at an angle of about 43^o. As the spacecraft spins the star image moves across the reticle forming a pulse train which is telemetered to the ground. The measurement of times when stars transit the vertical and slanted slits together with the identification of the stars provide enough information to deduce the inertial orientation of the spacecraft. For the present experiment inertial attitude has been obtained to an accuracy (1σ) of 0.01^o.

Telemetry

An FM-FM telemetry system was used to transmit data from the radiometer in real time. Since a total of 10 detector signals are transmitted, each side of the radiometer used a separate carrier frequency to allow sufficient bandwidth for all data channels. Frequency bandwidth requirements for the star mapper precluded the use of a subcarrier so a third carrier frequency was used which was directly modulated by the star-mapper output signal.

Calibration

Both the CO_2 and H_2O sides of the radiometer were calibrated by alternately viewing two black-body sources through an optical system such that the sources appeared extended and at infinity. One source was maintained at 77^o K (essentially zero radiance to the radiometer) while the second was varied from 77^o K to 250^o K. All calibrations were

done in a vacuum to eliminate absorption by CO_2 and H_2O. The absolute reflectance of the optical system used to relay the energy from the source to the radiometer was determined by measuring the reflectance of small optical flats coated in the chamber with the optics.

DATA REDUCTION

All data were recorded as a function of time during flight. In postflight reduction, tangent height and radiance data were each processed as a function of time and then combined to form radiance profiles.

Radiance Data

In radiometric calibration each detector was calibrated with the black-body sources, and a radiance responsivity k was determined from the following equation:

$$V = k \int \left[N_{\bar{\nu}}(T) - N_{\bar{\nu}}(77^{\circ}\,K) \right] \varphi(\bar{\nu})\, \rho(\bar{\nu})\, d\bar{\nu} \tag{1}$$

The purpose of the experimental measurement was to deduce the radiance of the horizon profile in some spectral band given by

$$N(H) = \int_{\bar{\nu}_1}^{\bar{\nu}_2} N_{\bar{\nu}}(H)\, d\bar{\nu} \tag{2}$$

A calculation of N(H) from a measurement of V requires a knowledge of the spectral shape of $N_{\bar{\nu}}(H)$. It has been assumed that the analytically computed shape of $N_{\bar{\nu}}(H)$ is correct. The 1962 U.S. Standard Atmosphere (ref. 9) has been used with the water vapor mixing ratio of reference 2, atmosphere A. The equation used to compute N(H) is

$$N(H) = \frac{V}{k} \left[\frac{\int_{\bar{\nu}_1}^{\bar{\nu}_2} N_{\bar{\nu}}(H)\, d\bar{\nu}}{\int N_{\bar{\nu}}(H)\, \varphi(\bar{\nu})\, d\bar{\nu}} \right] \tag{3}$$

Wave-number limits are 615 cm^{-1} to 715 cm^{-1} in the CO_2 band and 315 cm^{-1} to 475 cm^{-1} in the H_2O band. Actually, the ratio of the integrals in equation (3) varies with tangent height H. It is desirable to present radiance data independent of the measuring instrument but also to alter the raw data as little as possible. For these reasons, the integral ratio in equation (3) was evaluated at one value of H for CO_2 and one for H_2O to give a single constant in each band to convert voltage to radiance. For CO_2, the 1962

U.S. Standard Atmosphere at H = 20 km was used. In the H_2O band, the U.S. Standard Atmosphere with the mixing ratio of reference 2 atmosphere A at H = 15 km was used.

Accuracies of the radiometric measurement are given in the following table. All radiance data presented for the CO_2 band is obtained by averaging the radiance data from four detectors; thus, accuracies for CO_2 are also based on averaged data. Relative accuracy is the accuracy of the data from one profile to another profile or points within one profile. The radiometric accuracy near maximum values of radiance is 4 to 5 percent for both CO_2 and H_2O radiance data.

Radiance, W/m^2-sr	Absolute accuracy (1σ), percent		Relative accuracy (1σ), percent	
	CO_2	H_2O	CO_2	H_2O
12		4 to 5		3 to 4
6	4 to 5	7 to 8	2 to 3	6 to 7
3	6 to 7		4 to 5	

Tangent Height

Tangent height is defined (fig. 8) as the distance along a geocentric radius vector from the surface to the point where the radius vector is normal to the line of sight which originates at the spacecraft. Determination of tangent height as a function of time requires a knowledge of several parameters. These parameters and their source of information are as follows:

Parameter	Source
Inertial orientation of spacecraft	Star mapper
Angular position of radiometer line of sight	Position points of scan mirror
Altitude, latitude, and longitude of spacecraft	Radar
Earth shape	Fisher spheroid
Time	Time generator on ground

These data when combined are estimated to yield tangent height accuracy (1σ) of 1.5 km.

DATA PRESENTATION

Geographical location of horizon scans presented is shown in figure 9. A circle with a cross inside denotes the location of analytical radiance profiles generated independently of the measured radiance profiles. Locations of measured radiance profiles are shown as solid bars for those in the CO_2 band and as dashed bars for the H_2O band.

The measured profiles are spread geographically due to spin rate and the time necessary to cross the horizon; length of the bars is indicative of the amount of spread experienced. Latitude coverage of the experiment is seen to be from 15^{o} N to 55^{o} N.

Meteorological Rocket Network Support

Four meteorological rocket network (MRN) sites made special launchings to measure temperature, wind speed, and wind direction in support of the experiment. All MRN data were gathered within 2 hours of horizon data. The MRN data were combined with balloon data below 30 km to infer atmospheric temperature distributions in regions where horizon crossings occurred. Inference of temperature distributions was made by means of the thermal wind technique as discussed in reference 10. The resulting temperature data were used in analytical calculations of horizon profiles to compare with measured profiles. The MRN sites are shown in figure 9 to be Ft. Churchill, Manitoba; White Sands, New Mexico; Wallops Island, Virginia; and Eglin Air Force Base, Florida.

Analytical Profiles for CO_2 Band

The theoretical model for the calculated profiles in the CO_2 band is discussed in reference 4. Effects of refraction, Doppler broadening, and absence of local thermodynamic equilibrium have been included. All profiles have been computed for a CO_2 concentration of 314 parts per million. Figure 10 shows the analytical radiance profiles and temperature distributions at the extremes in latitude of the experimental data. Meteorological conditions result in analytically predicted radiance profiles with differences of 0.7 W/m^2-sr in peak radiance due to tropospheric temperature variations but little difference in radiance levels at larger tangent heights as seen in figure 10. Temperature variations with latitude which are large for low altitudes but small at higher altitudes are not unusual for the summer season. Analytical profiles for the 615 cm^{-1} to 715 cm^{-1} band used in comparison with measured data are shown as dashed curves in figure 11.

Measured Profiles for CO_2 Band

Measured radiance profiles in the 615 cm^{-1} to 715 cm^{-1} interval are shown in figure 11 as solid curves. All radiance data for this spectral interval were obtained by averaging data from four detectors. These radiance profiles are typical examples of the experimental data and cover the latitude range of the experiment. Figure 11(a) shows a comparison of a measured and analytical radiance profile for the southern limit of the experimental data. Agreement between the two curves is remarkable. Radiance differences near peak radiance are less than the experimental error previously stated. Figures 11(b), (c), and (d) illustrate similar comparisons in other geographic locations. In the region of 30 km to 40 km all data show extremely good agreement. Above 45 km

the agreement is not as good in figures 11(c) and (d) as in figures 11(a) and (b). Differences however do not exceed errors of the measurement and analytical prediction. This excellent agreement between measured and analytical data verifies the analytical technique used to compute radiance profiles in the 615 cm^{-1} to 715 cm^{-1} region to within the accuracy of the experiment.

It should be noted that the horizon profiles in all cases are formed at tangent heights higher than 15 km. These radiance profiles will be affected little by tropospheric weather variations. The agreement of measured and analytical profiles and the lack of dependence on weather variations indicate the spectral region of 615 cm^{-1} to 715 cm^{-1} is an excellent choice for horizon sensing to aid in attitude determination.

Measured Profiles for H_2O Band

Experimentally measured radiance profiles from a single detector in the 315 cm^{-1} to 475 cm^{-1} interval are presented in figure 12. No analytical profiles are presented for the H_2O band since the H_2O mixing ratio in the atmosphere was not known independently of the profile measurement.

Three radiance profiles are shown. The profiles at latitude 13° N and at 57° N are examples near the extremes of the latitude coverage of the experiment. They are remarkably similar considering the variability of H_2O in the atmosphere. Radiance levels less than 2 W/m^2-sr above 20 km evident in all the curves are an indication of a dry atmosphere above 20 km. The very steep slope of 1.2 W/m^2-sr-km from 15 km to 5 km is indicative of a rapidly changing mixing ratio of H_2O. In fact the steep slope is scanned too rapidly and the radiometer frequency response has been exceeded. Larger radiance levels (>7 W/m^2-sr) are distorted by frequency limitations of the system.

The third profile at latitude 39° N in figure 12 is a dramatic example of the effect clouds can have on a radiance profile. A cloud at 10 km to 12 km has produced a radiance of 5.7 W/m^2-sr at 5 km compared with one greater than 10 W/m^2-sr for the other profiles. Cloud effects of this magnitude are highly undesirable for applications in horizon sensing for attitude determination and will make the 315 cm^{-1} to 475 cm^{-1} region a poor one to use for high accuracy attitude determination.

It should also be noted that the CO_2 profile in figure 11(c) is in the same geographic region as the cloudy profiles but was unaffected by the cloud since the entire profile originated above the cloud height.

CONCLUDING REMARKS

Measured horizon radiance profiles in the 615 cm^{-1} to 715 cm^{-1} spectral region (CO_2) are formed high enough in the atmosphere to be affected little by tropospheric

weather variations; thus, the spectral region should be a good one for use in attitude determination applications. The excellent agreement between measured profiles and analytically predicted profiles has verified the analytical technique within the accuracy of the experiment for the 615 cm^{-1} to 715 cm^{-1} region. Measured horizon profiles in the 315 cm^{-1} to 475 cm^{-1} region (H_2O) show a strong dependence on clouds; therefore, this spectral region would not be a good candidate for aid in attitude determination.

Langley Research Center,
National Aeronautics and Space Administration,
Langley Station, Hampton, Va., September 22, 1967,
715-02-00-01-23.

REFERENCES

1. Hanel, R. A.; Bandeen, W. R.; and Conrath, B. J.: The Infrared Horizon of the Planet Earth. J. Atmospheric Sci., vol. 20, no. 2, Mar. 1963, pp. 73-86.

2. Wark, D. Q.; Alishouse, J.; and Yamamoto, G.: Variation of the Infrared Spectral Radiance Near the Limb of the Earth. Appl. Opt., vol. 3, no. 2, Feb. 1964, pp. 221-227.

3. Duncan, John; Wolfe, William; Oppel, George; and Burn, James: Infrared Horizon Sensors. 2389-80-T (Contract NOnr 1224(12)), Inst. Sci. Technol., Univ. of Michigan, Apr. 1965. (Available from DDC as AD 466289.)

4. Bates, Jerry C.; Hanson, David S.; House, Fred B.; Carpenter, Robert O'B.; and Gille, John C.: The Synthesis of 15μ Infrared Horizon Radiance Profiles From Meteorological Data Inputs. NASA CR-724, 1967.

5. Jalink, Antony, Jr.: An Investigation of the Earth's Horizon in the Infrared. M. Elec. Eng. Thesis, Univ. of Virginia, 1966.

6. Walker, R. G.; Cuniff, C. V.; and D'Agati, A. P.: Measurement of the Infrared Horizon of the Earth. AFCRL-66-631, U.S. Air Force, Sept. 1966.

7. Dodgen, J. A.; McKee, T. B.; and Jalink, A.: NASA-LRC Program To Define Experimentally the Earth's IR Horizon. NASA paper presented at the Symposium on Infrared Horizon Sensors for Spacecraft Guidance and Control (El Segundo, Calif.), Mar. 14-15, 1967.

8. Garner, H. D.; and Reid, H. J. E., Jr.: Simulator Studies of Simple Attitude Control for Spin-Stabilized Vehicles. NASA TN D-1395, 1962.

9. Anon.: U.S. Standard Atmosphere, 1962. NASA, U.S. Air Force, and U.S. Weather Bur., Dec. 1962.

10. Peterson, Roy E.; Schuetz, John; Shenk, William E.; and Tang, Wen: Derivation of a Meteorological Body of Data Covering the Northern Hemisphere in the Longitude Region Between 60^{o} W and 160^{o} W From March 1964 Through February 1965. NASA CR-723, 1967.

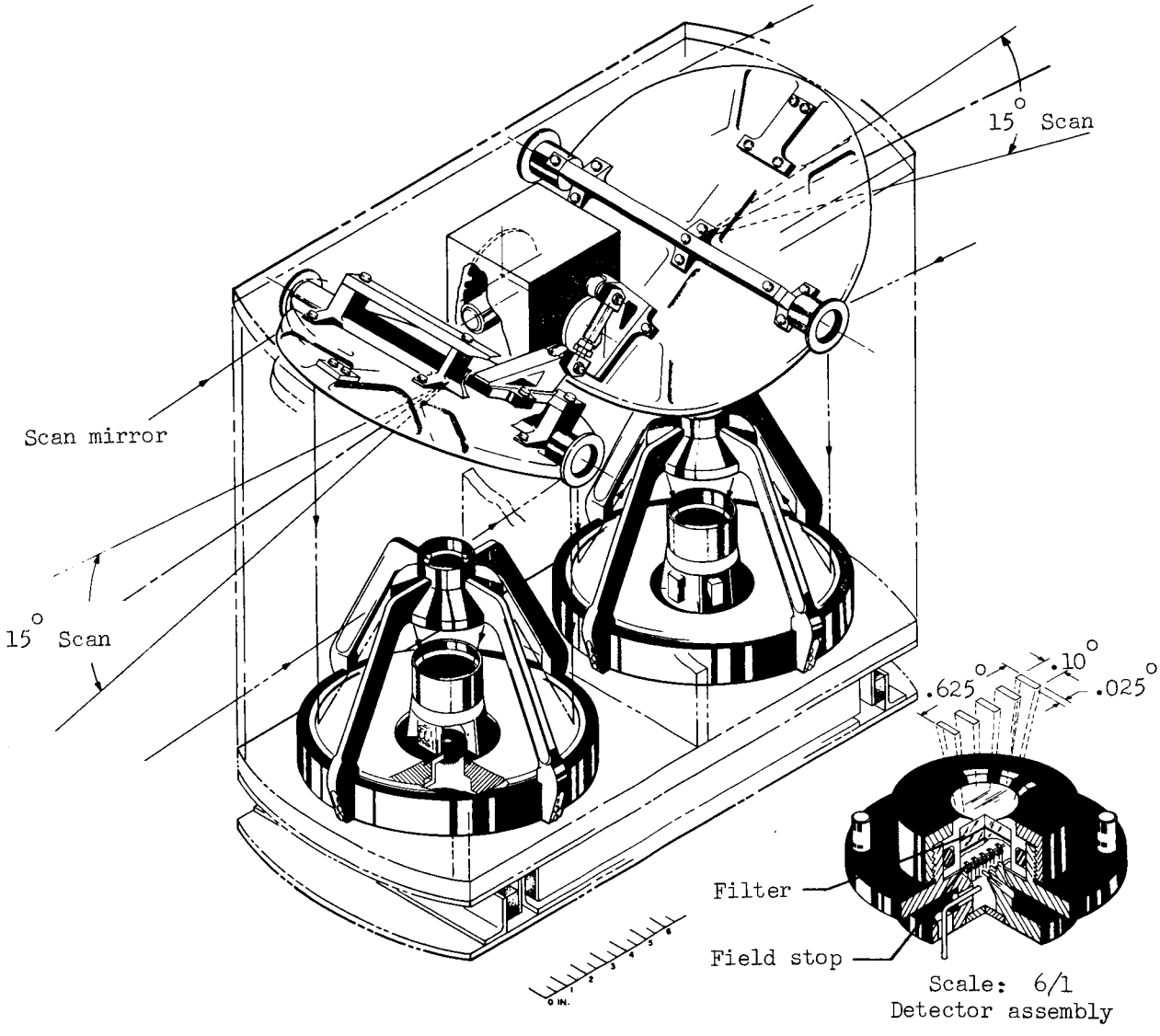

Figure 1.- Sketch of dual radiometer.

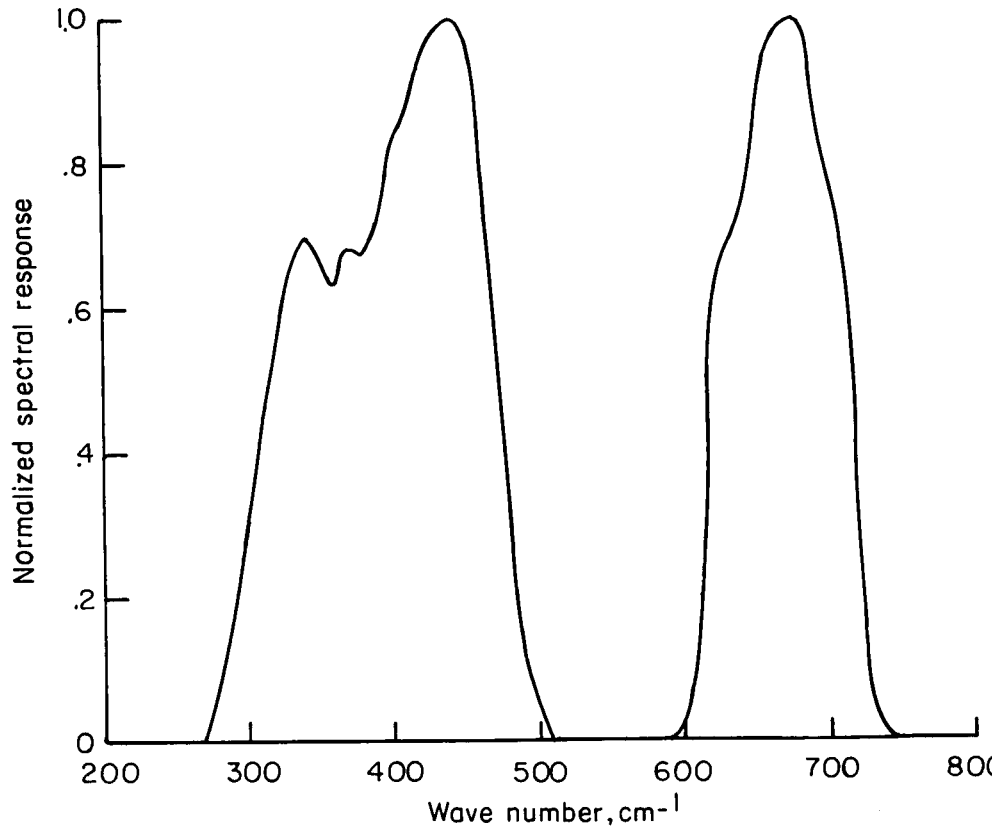

Figure 2.- Normalized dual-radiometer spectral response.

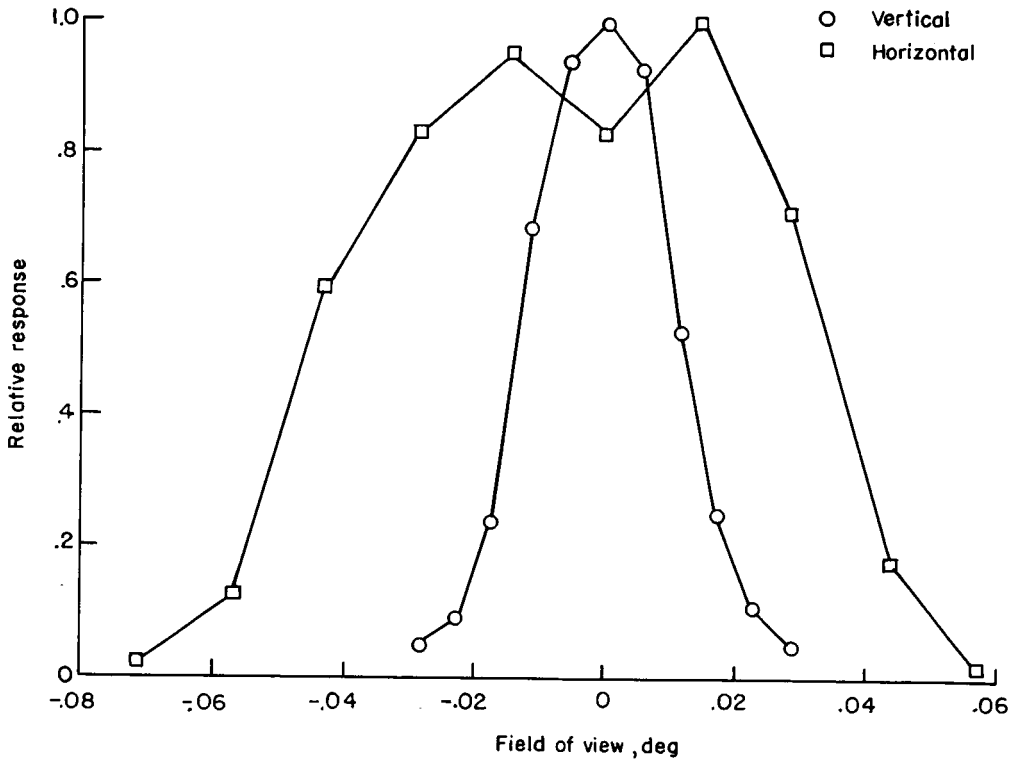

Figure 3.- Typical field of view contour for 615 cm^{-1} to 715 cm^{-1} radiometer.

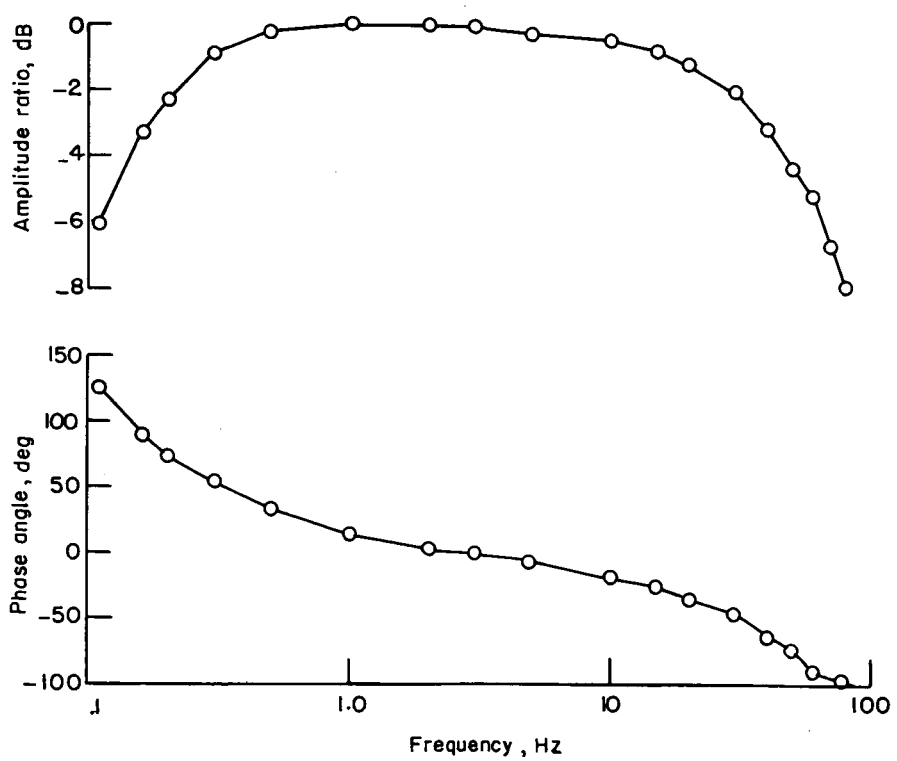

Figure 4.- Typical phase and amplitude response for 615 cm^{-1} to 715 cm^{-1} radiometer.

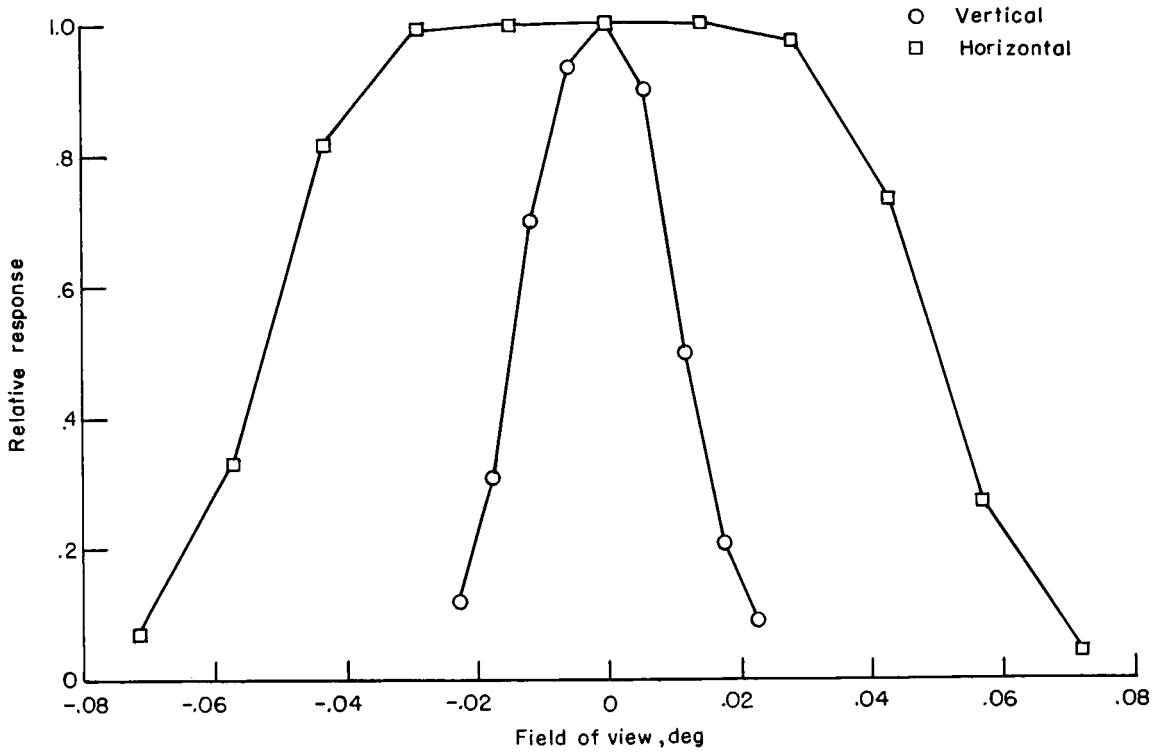

Figure 5.- Typical field of view contour for 315 cm^{-1} to 475 cm^{-1} radiometer.

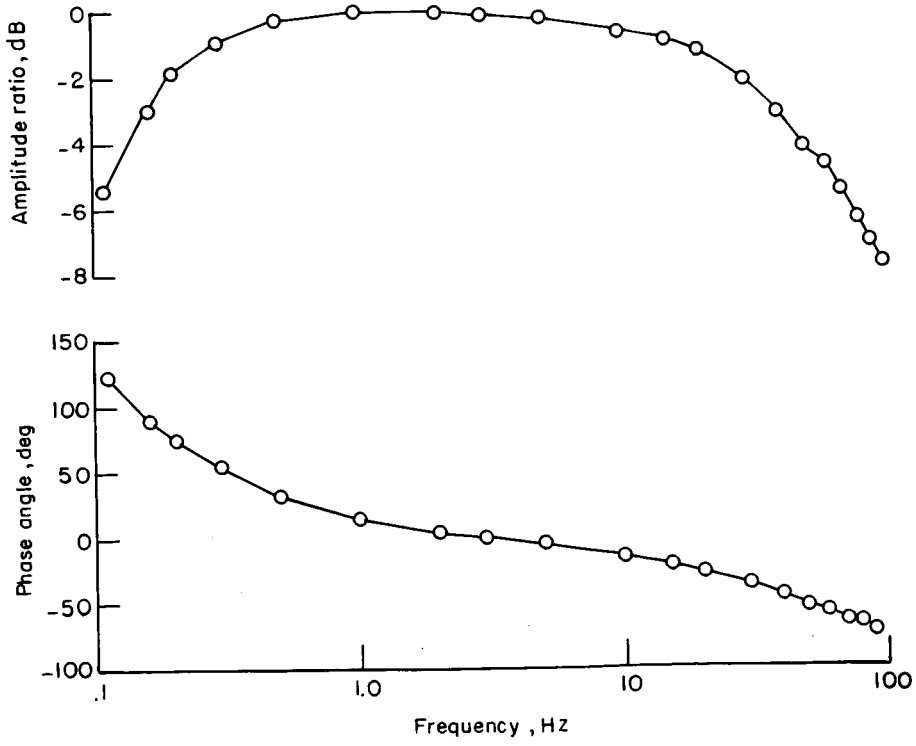

Figure 6.- Typical phase and amplitude response for 315 cm^{-1} to 475 cm^{-1} radiometer.

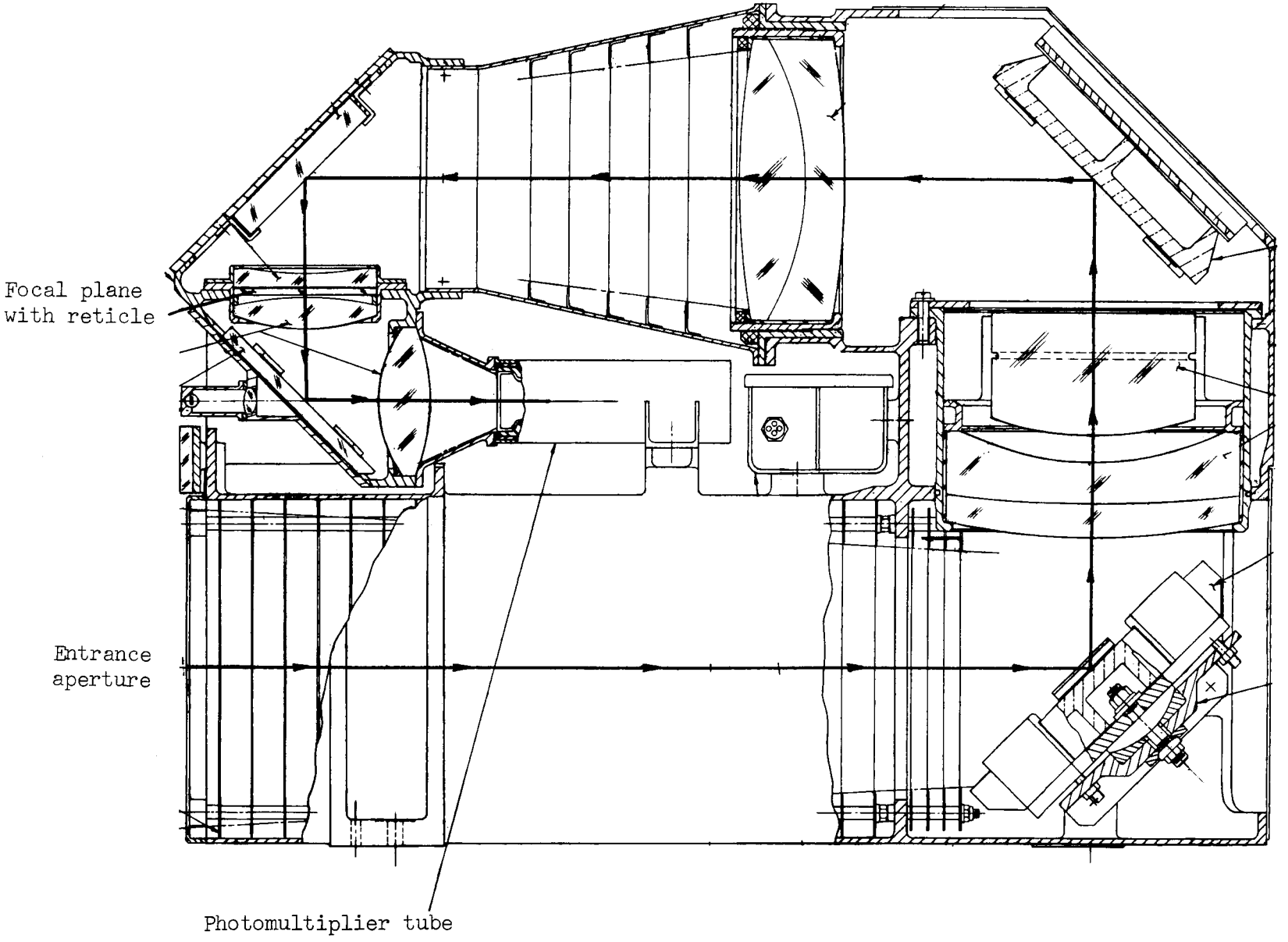

Figure 7.- Sketch of star mapper.

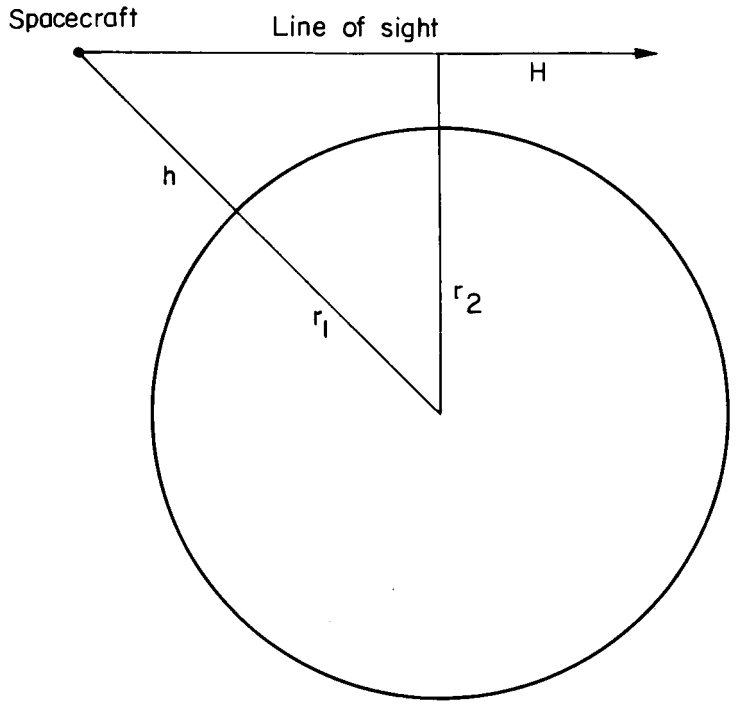

Figure 8.- Definition of tangent height H.

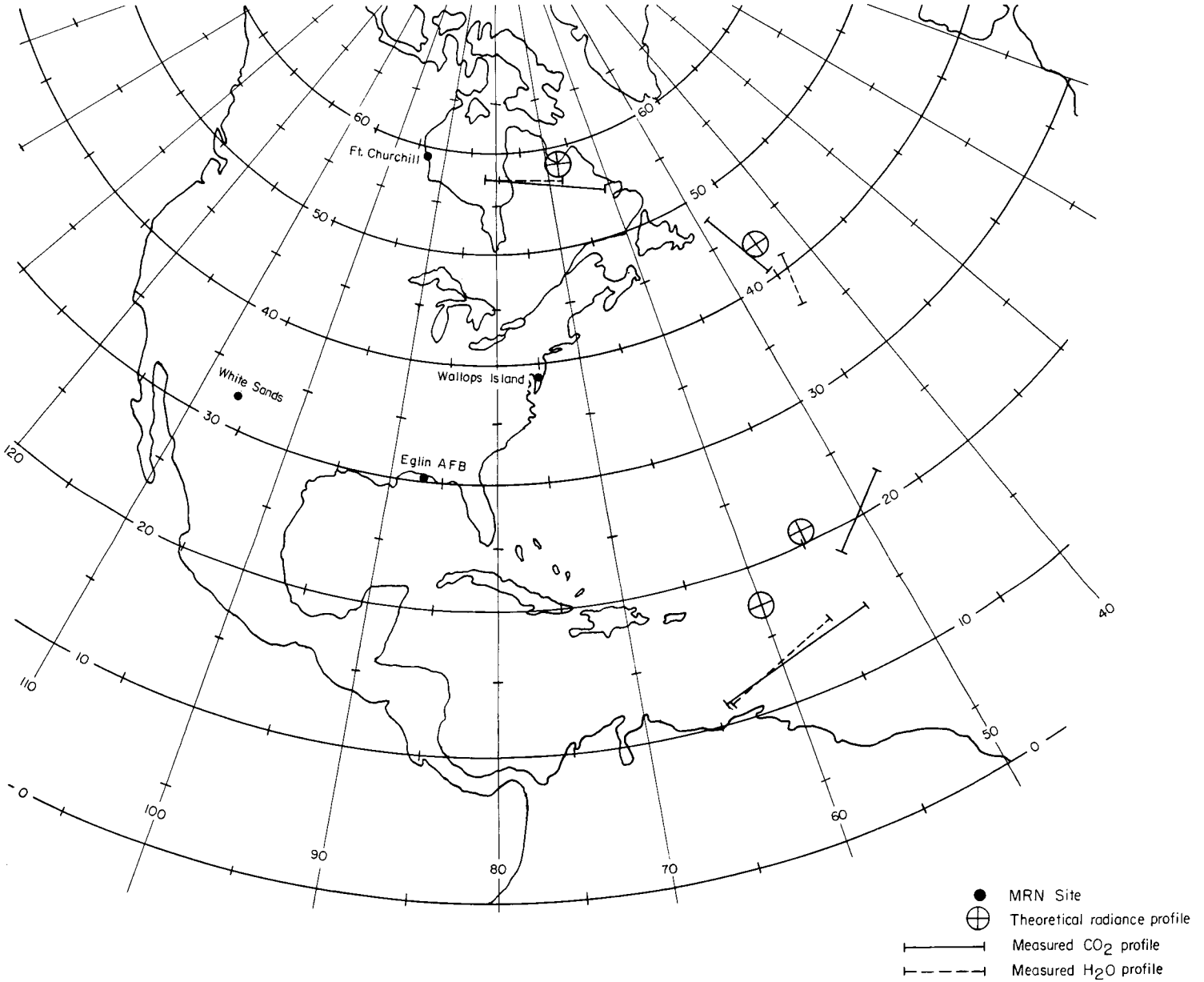

Figure 9.- Geographic location of horizon crossings and MRN sites.

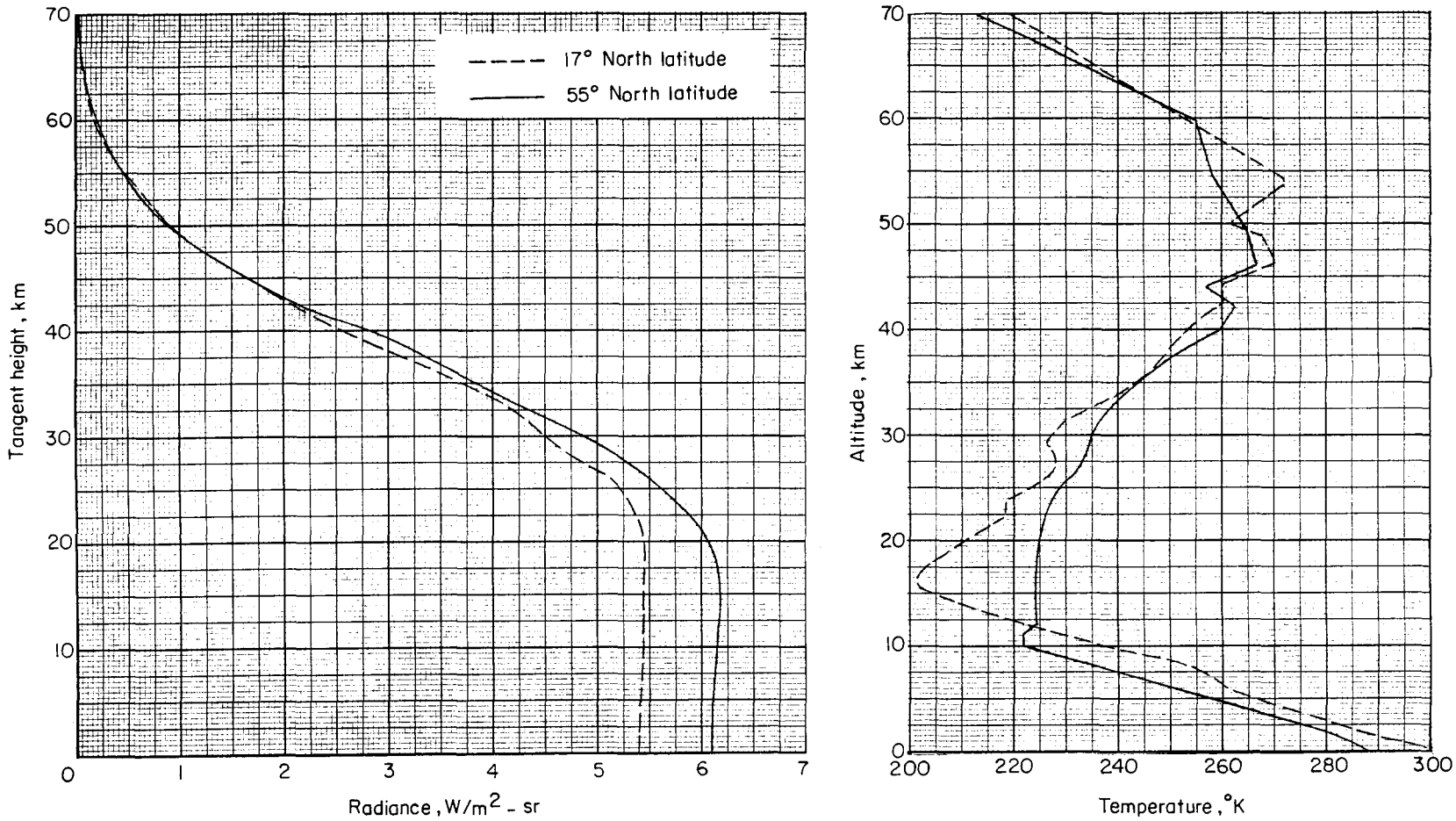

Figure 10.- Comparison of analytical radiance profiles in 615 cm^{-1} to 715 cm^{-1} band and temperature profiles for extremes in latitude.

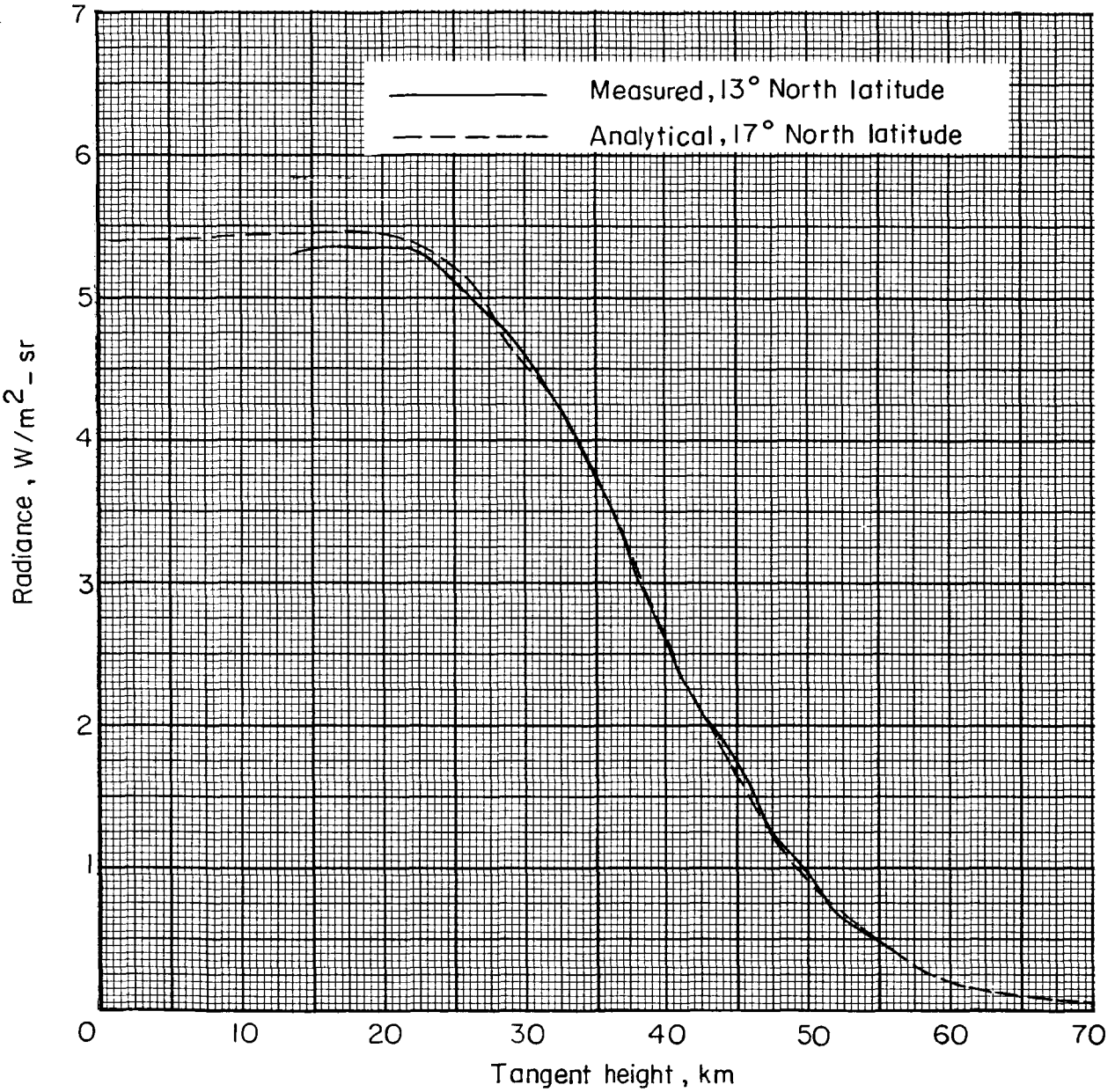

(a) Near latitude 13^0 N.

Figure 11.- Comparison of measured and analytical radiance profiles in 615 cm^{-1} to 715 cm^{-1} band.

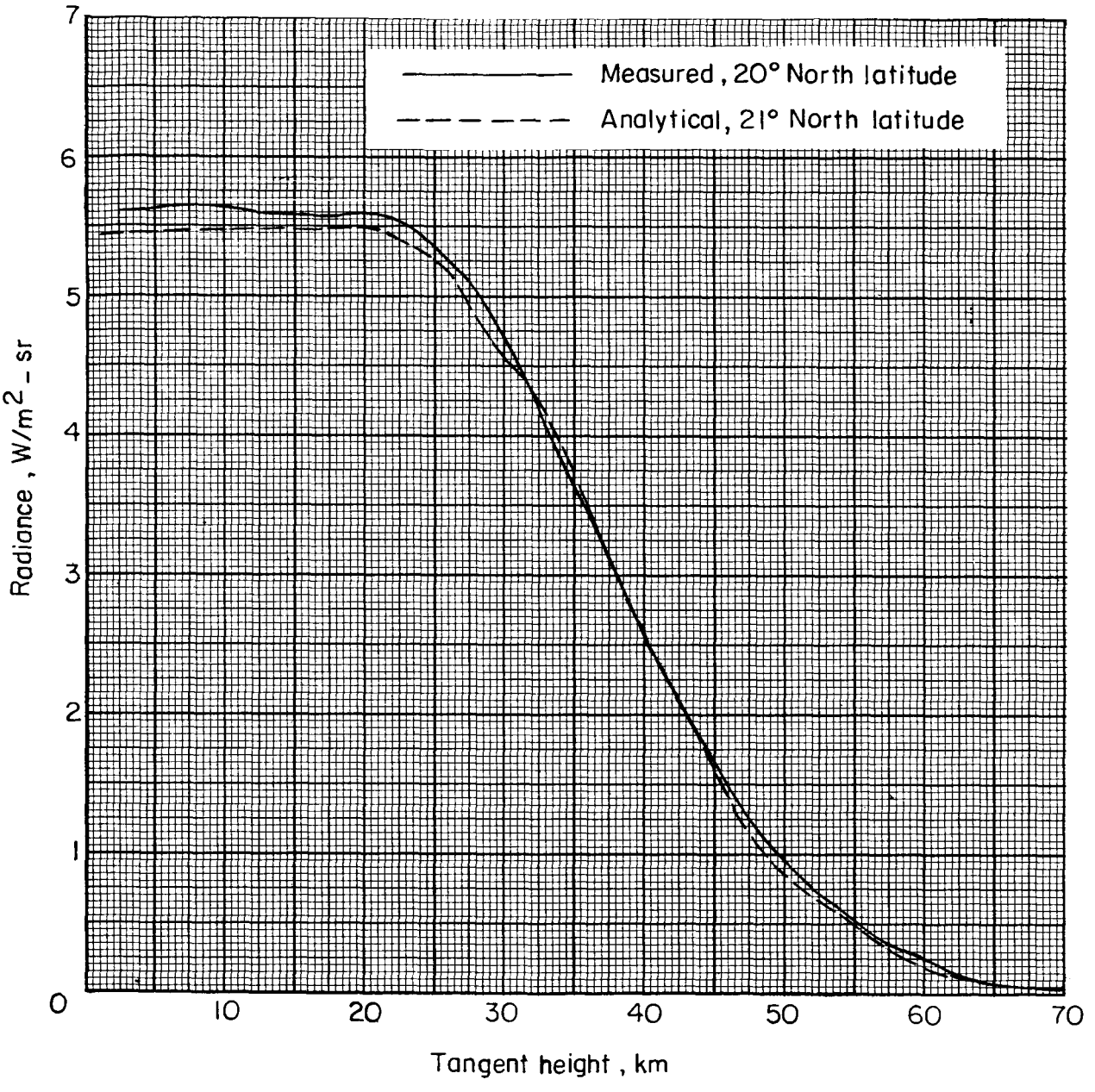

(b) Near latitude 20^0 N.

Figure 11.- Continued.

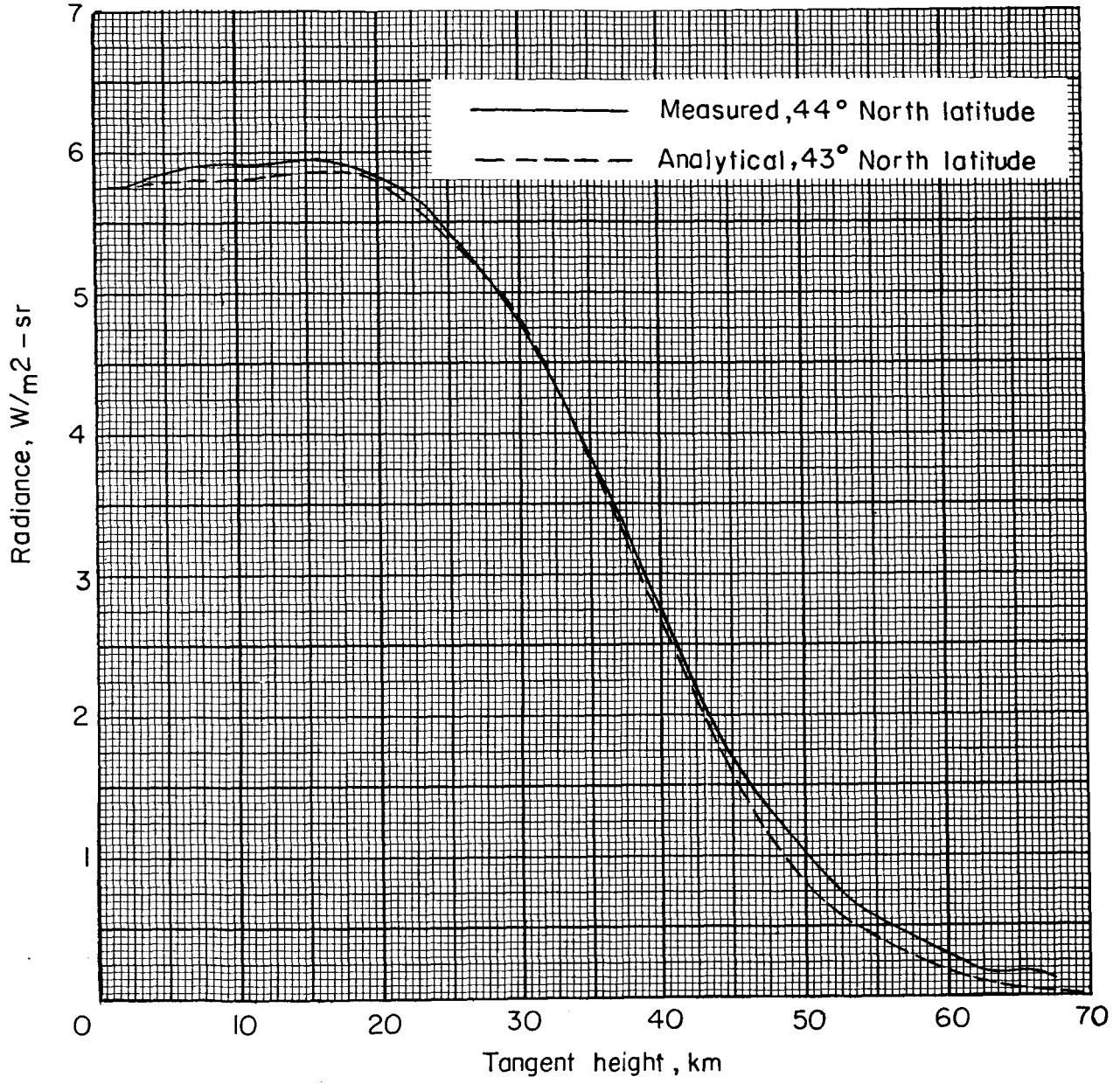

(c) Near latitude 44° N.

Figure 11.- Continued.

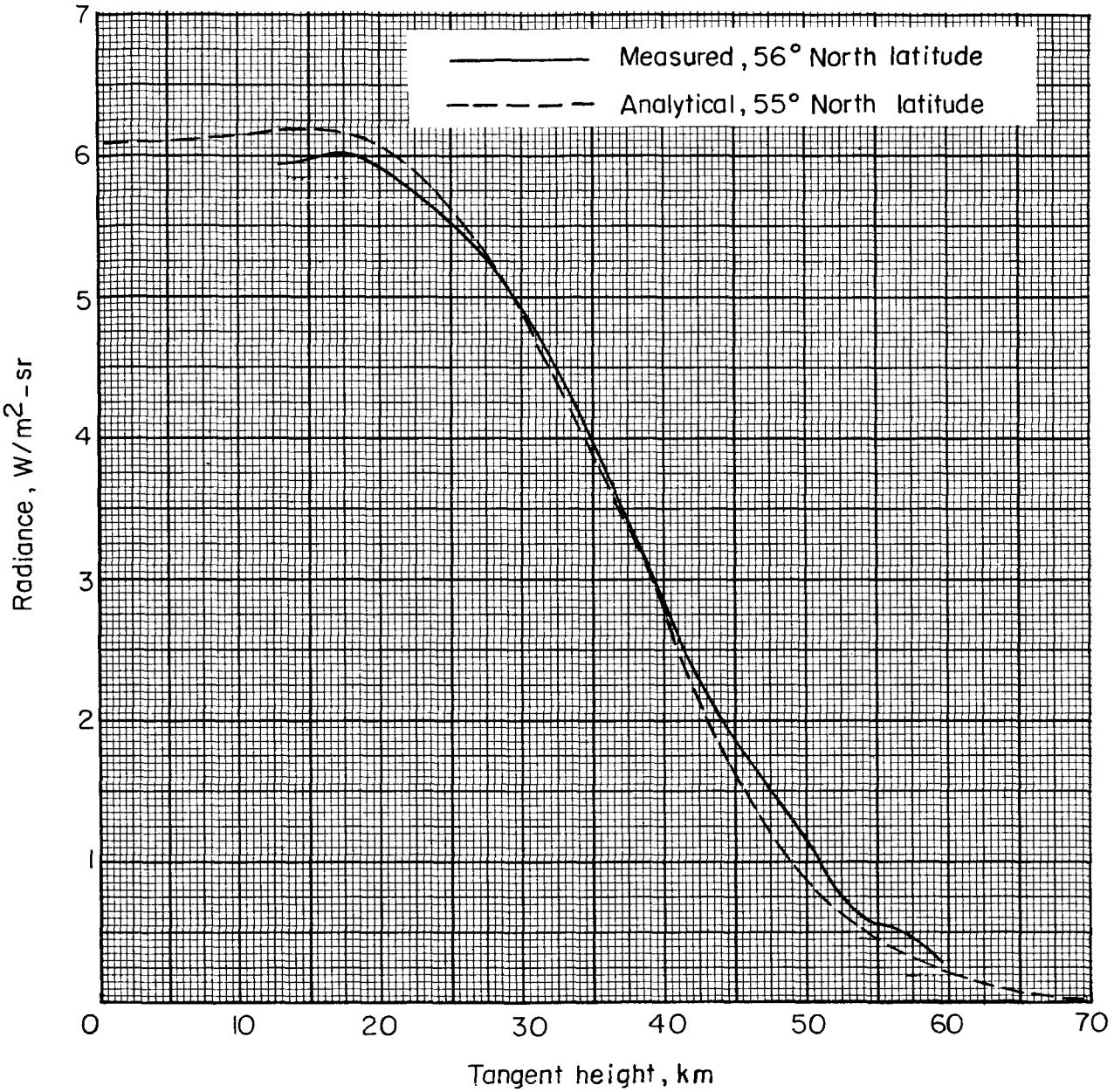

(d) Near latitude 56^0 N.

Figure 11.- Concluded.

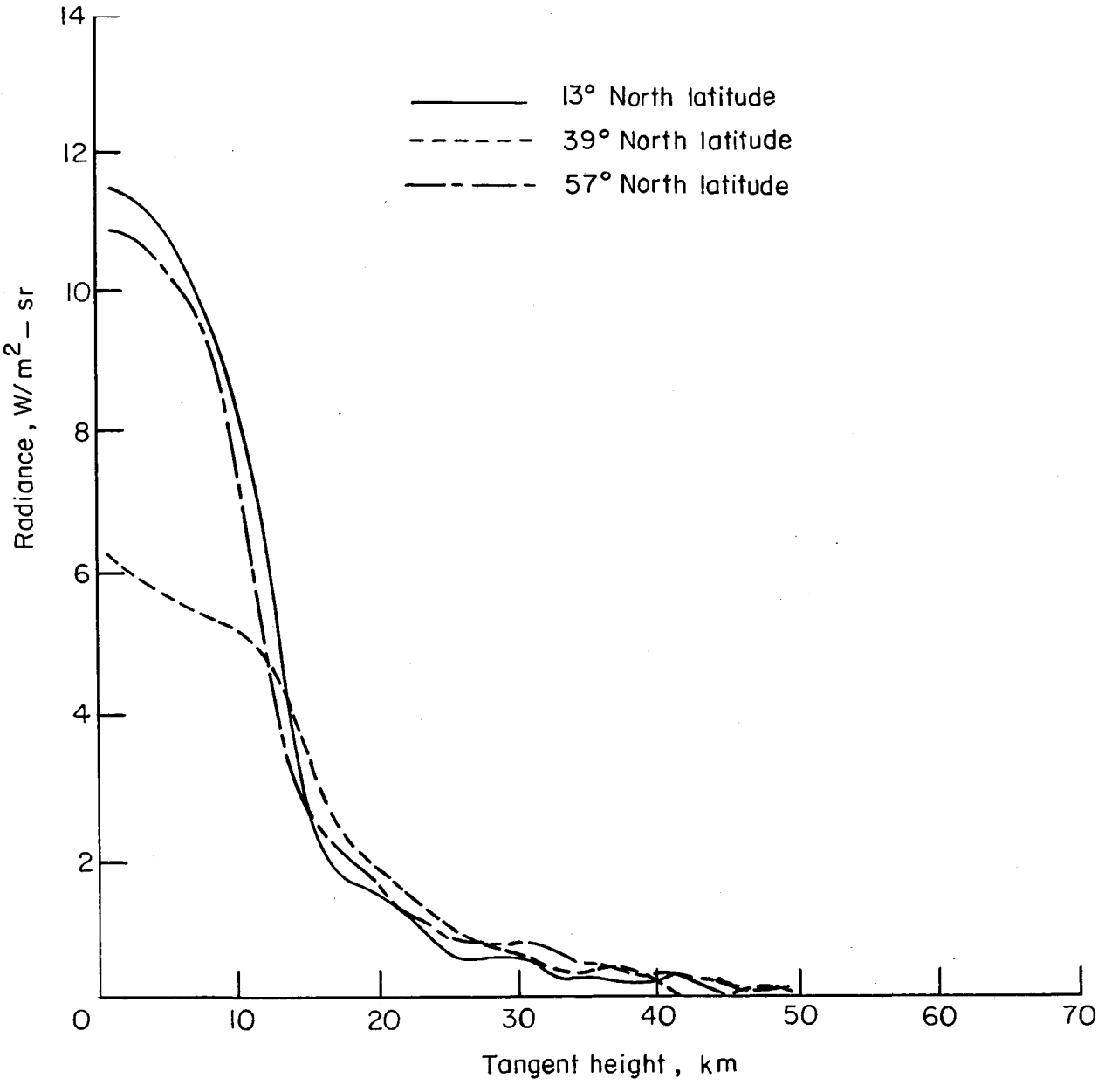

Figure 12.- Measured radiance profiles in 315 cm^{-1} to 475 cm^{-1} band.